Journal of Electroceramics, 14, 193–198, 2005

Microstructural and High-Temperature Electrical Characterization of $La_{1-x}Sr_xFeO_{3-\delta}$

EDWARD V. BONGIO,* HAMILTON BLACK, FABIENNE C. RASZEWSKI, DOREEN EDWARDS, CASPAR J. McCONVILLE & VASANTHA R.W. AMARAKOON

New York State College of Ceramics, Alfred University, Alfred, NY, USA

Submitted March 5, 2003; Revised October 14, 2004; Accepted November 5, 2004

Abstract. Strontium-doped lanthanum ferrites (LSF) were studied using scanning electron microscopy (SEM), X-ray diffraction (XRD), 4-point D.C. electrical conductivity and bulk property measurements. The results were compared to those of previous studies as well as selected processing conditions. The investigation focused on effects of sintering temperature, time, atmosphere (air, O_2 and N_2) and composition of $La_{1-x}Sr_xFeO_{3-\delta}$ ($x = 0.2$–0.9), on the sintering behavior, microstructural development and electrical conductivity. An oxalate precipitation method was used to prepare lanthanum ferrite powders. Simultaneous thermogravimetric and differential thermal analysis (TGA/DTA) studies found calcination temperatures of 800 and 850°C were necessary to form single-phase crystalline powders, as determined by XRD. Specimens were sintered from 1300 to 1400°C with dwell times from $\frac{1}{2}$ to 2 hrs. Results from SEM/EDS analysis showed the presence of a second phase in the samples fired in air or oxygen. The second phase was not detected by x-ray diffraction due to the small amount of material present. Samples fired in nitrogen had the lowest conductivity while those fired in oxygen had the highest. A composition of $x = 0.5$ resulted in the highest conductivity, 352 S/cm, at an operating temperature of 550°C in air. High strontium additions ($x = 0.9$) lowered the linear shrinkage of LSF.

Keywords: SOFC, cathode, microstructure, electrical conductivity, lanthanum strontium ferrite

1. Introduction

Fuel cells are relatively new, environmentally friendly devices for the production of electrical power. A fuel cell consists of a cathode, typically an ABO_3 (A = La, Sr, Ca) (B = Fe, Mn, Co) perovskite, an electrolyte (yttrium stabilized zirconia (YSZ)), and an anode (Ni-YSZ cermet) [1, 2]. Strontium-doped lanthanum ferrites (LSF), $La_{1-x}Sr_xFeO_{3-\delta}$, are candidate materials as cathodes for high-temperature solid oxide fuel cells as they have been found to have sufficient *p*-type electrical conductivity [3] (>100 S/cm). While there are several studies and reviews published [3–8] that report the effects of A and B site doping, there is little information regarding the effects of processing conditions on $La_{1-x}Sr_xFeO_{3-\delta}$ properties. The effect of temperature on the electrical conductivity of $La_{1-x}Sr_xFeO_{3-\delta}$ is also well understood [1–7, 9] and has been described in terms of small-polaron hopping conduction for LSF, but again the results have not been closely related to processing conditions. As a result there is little agreement in published literature as to the effects of processing variables on cathode properties [10] or microstructure.

It is the intent of this paper to study the influence of processing conditions on the electrical properties and microstructure of LSF perovskites. Specifically, the sintering temperature, time and atmospheric conditions have been investigated.

Bell determined that an oxalate precipitation synthesis technique produced the best material for oxygen catalysis [11] in SOFC operating conditions in comparison to citrate, sol-gel or carbonate derived materials. As a result, a modified oxalate precipitation process, described by LaCourse [12], was used to synthesize

*To whom all correspondence should be addressed. E-mail: bongioe@starfiresystems.com

materials for this study. Dann et al. studied the effect of oxygen stoichiometry on phase relations in LSF and concluded that only in high-pressure oxygen does a phase-pure composition always form [13]. Based on the operating conditions of cathode materials and the study by Dann et al. the partial pressure of oxygen (PO_2) has a significant effect on phase evolution. Therefore varying the PO_2, by sintering in flowing air, O_2 or N_2 during firing, was chosen as a processing variable. Literature [3, 4] does not agree on how sintering temperatures affect the microstructure and properties of cathode materials. Minh found that upon raising the firing temperature of $LaMnO_3$ the interfacial resistance between the cathode and electrolyte increases due to smoother particle formations [1]; Simner suggests optimized firing conditions for $La_{0.8}Sr_{0.2}FeO_3$ of 1150°C for 2 h [4]; and Raszewski studied $La_{0.1}Sr_{0.9}FeO_{3-\delta}$ and found that temperatures greater than 1400°C or at long dwell times at 1400°C the samples will fracture during cooling [14]. Therefore firing time and temperature have been chosen as significant processing variables having an effect on the electrical conductivity.

Typical values for electrical conductivity were found by Kim et al. and show the trend of increasing x to 0.5 increases conductivity while further increases of x decrease the conductivity [7]. Meixner and Cutler found that increasing x decreased the density and prevented sintering in lanthanum strontium manganites [8]. Therefore the last processing variable chosen was the composition of LSF. The composition range varied from $x = 0.2$ to 0.9.

2. Experimental Procedure

2.1. Oxalate Precipitation

The $La_{1-x}Sr_xFeO_3$ materials, where $x = 0.2, 0.5, 0.7, 0.9$, were prepared using a modified oxalate coprecipitation method [12]. A 0.45 molal metal nitrate solution was made using deionized H_2O and stochiometric amounts of $Sr(NO_3)_2$(99 + %, Aldrich Chemical Co., Milwaukee, WI), $La(NO_3)_3{\cdot}6H_2O$ (99.9%, Aldrich), and $Fe(NO_3)_3{\cdot}9H_2O$ (98 + %, Aldrich). The nitrate solution was added in 50 mL increments using a 50 mL burette into a 0.6 molar oxalic acid (99%, Aldrich) solution held at 50°C. Precipitation of an oxalate complex was apparent with the formation of a yellow precipitate. After the metal nitrate solution addition, the temperature was raised to 110°C. At 110°C a brown gas, assumed to be nitrogen dioxide, was evolved and excess water was occasionally added to the condensed solution until evolution of the brown gas ceased. The remaining bright yellow-green precipitate was placed in a Teflon beaker, and dried overnight at 100°C. Simultaneous thermogravimetric and differential thermal analysis (TGA/DTA) results were examined to determine temperatures for calcination steps for the oxalate precipitate powders.

The precipitate was heated once at 800°C for 15 h, crushed and mixed in a mortar and pestle; then calcined at 850°C for 8 h to form a single phase crystalline powder as determined by powder X-ray diffraction (XRD). Binder and plasticizer (1 wt% PVA and 0.3% PEG) were added to the calcined powders by ball milling with zirconia media for 1 h after which the slurry was dried at 80°C overnight. The dried powder was crushed and passed through a 212 μm mesh sieve. The powders were uniaxially pressed at 34.5 MPa; the pressure was released and then brought up to 68.9 MPa for 30 sec. Pellets were heated at 5 K/min to 600°C, kept at 600°C for 1 h for binder burnout and then sintered at temperatures from 1300 to 1400°C for 15 min to 2 h dwell times with a flowing atmosphere of N_2, air or O_2 at 500 mL/min.

2.2. Characterization

Thermal analysis was performed on the oxalate-precipitated powder using a simultaneous TGA/DTA analyzer (SDT 2960, TA Instruments, Inc., New Castle, DE) at 10 K/min ramp rate to 1100°C. Linear shrinkage was measured using a hot-stage microscope (Misura, Expert System, Modena, Italy) at a rate of 5 K/min; taking measurements every 1 K from 600 to 1450°C.

XRD was performed on sintered samples with a polished surface and on powdered samples using Cu-Kα radiation from 20 to 70 2θ, with 0.04°C steps and 3 sec dwell on a powder X-ray diffractometer (XRG 3100 X-ray diffractometer, Philips, Eindhoven, Netherlands).

For electrical property measurements, rectangular bars (approximately, 3 mm × 3 mm × 15 mm) were cut from sintered pellets. The D.C. electrical conductivity was measured using a four-point method. The bar was compressed between two current-carrying outer electrodes (Pt foil), and the voltage drop was measured at two inner electrodes. Samples were ramped down at 3

K/min from 900 to 100°C and voltage measurements were taken after 1 h dwells at 100°C intervals for controlled atmosphere samples. Measurements were taken in the same atmosphere that the samples were sintered in with a flow rate of 500 mL/min. Electrical conductivity data were measured in 50°C steps with 10 min dwell times up to 1000°C with 10 K/min ramp rate for initial A-site doping studies.

Micrographs of the samples were taken using scanning electron microscopy (SEM) (SEM 515, Philips, Eindhoven, Netherlands) in secondary electron mode with energy dispersive X-ray spectrometry (EDS) to determine the chemical composition of phases present. Lastly, the Archimedes method was used on the N_2, O_2 and air sintered samples to determine open porosity, apparent porosity and bulk density.

3. Results

Thermal analysis data shows that the onset of shrinkage was approximately 1000°C and the final shrinkage was about 25% for $x = 0.2$, 0.5 and 0.7 where $x = 0.9$ obtained only 15% shrinkage.

Electrical conductivity, σ, vs. composition of $La_{1-x}Sr_xFeO_{3-\delta}$ from $x = 0.2$ to 0.9 is plotted in Fig. 1. The highest conductivity, 352 S/cm, was found at 550°C for a composition of $x = 0.5$ measured in air. At higher ($x > 0.5$) and lower ($x < 0.5$) levels of strontium addition the conductivity decreased. As the sintering temperature is increased from 1350 to 1400°C the maximum conductivity increases by a factor of 2 up to 302 S/cm for $x = 0.9$. Similar results were obtained for $x = 0.7$ while $x = 0.2$ and 0.5 compositions did not show as great an increase in conductivity with increasing sintering temperature. An increase in sintering time resulted in decreased electrical conductivities for samples with composition $x = 0.5$ sintered at 1400°C.

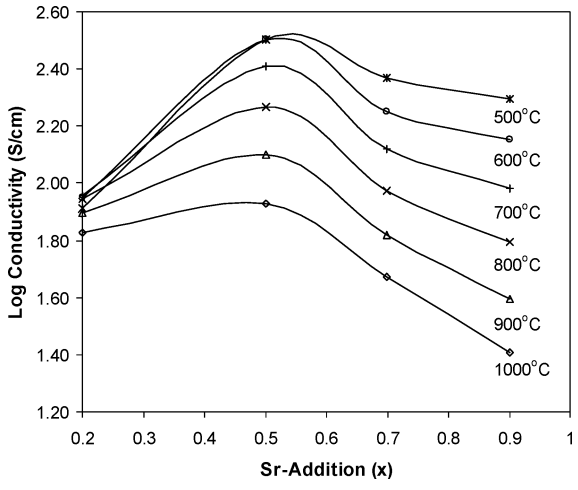

Fig. 1. Influence of strontium addition on σ at indicated temperatures where samples were sintered in flowing air at 1400°C for 1/2 h dwell and measurements were taken at 50°C intervals after 10 min dwell in air.

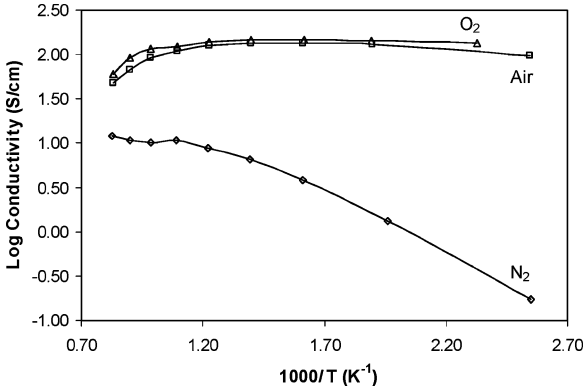

Fig. 2. Atmospheric dependence on σ for $La_{0.5}Sr_{0.5}FeO_3$ samples fired at 1400°C for 2 h in air, O_2 or N_2 with a constant flow rate of 500 mL/min.

The dependence of electrical conductivity on sintering atmosphere is shown in Fig. 2. The O_2 and air fired samples, of $x = 0.5$ composition, had electrical conductivities of 147 and 134 S/cm, respectively, at 450°C working temperatures. The N_2 sample shows a significant decrease in conductivity to only 7 S/cm at 450°C working temperature.

The density (4.966 g/cm^3) of $La_{0.5}Sr_{0.5}FeO_3$ increased and the apparent porosity (10.17%) decreased when sintered in N_2. Samples fired in O_2 had opposite results and achieved a density of 4.902 g/cm^3 and apparent porosity of 18.89%.

Micrographs of $x = 0.5$ samples sintered in flowing air and O_2 show the presence of a second, dark unknown phase as shown in Figs. 3 and 4 respectively. EDS data of the O_2 fired sample indicated that the "second phase" had a higher oxygen content and that the matrix phase had a higher strontium content than the air fired sample. The N_2 fired sample did not show second phase formation as shown in Fig. 5. EDS of the N_2 fired sample indicated large amounts of carbon as well as exaggerated levels of strontium. The detection of carbon by EDS suggests impurities were present on

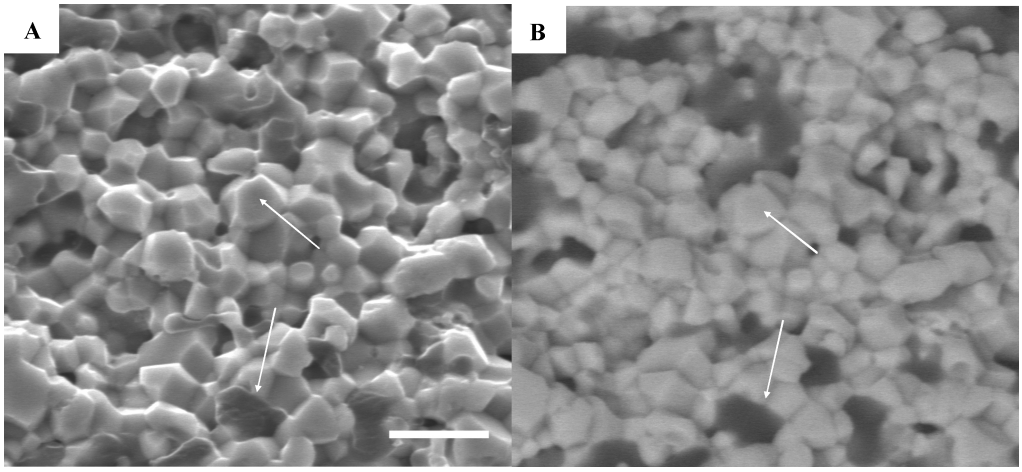

Fig. 3. Secondary (a) and backscattered electron (b) micrographs of $La_{0.5}Sr_{0.5}FeO_3$ sintered in flowing air with arrows pointing towards EDS analysis area with a 5 μm scale bar.

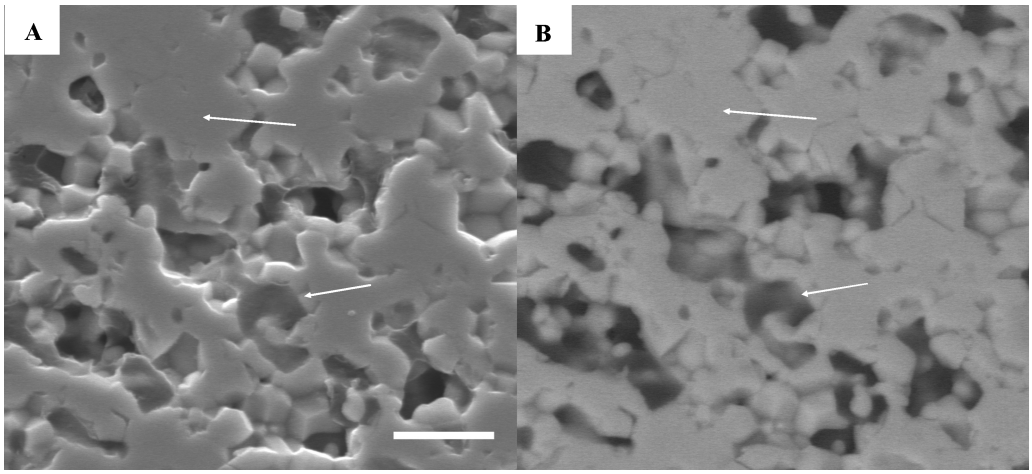

Fig. 4. Secondary (a) and backscattered electron (b) micrographs of $La_{0.5}Sr_{0.5}FeO_3$ sintered in flowing O_2 with arrows pointing towards EDS analysis areas with a 5 μm scale bar.

the sample surface. The presence of a second phase, in the $La_{0.5}Sr_{0.5}FeO_3$ air, N_2 or O_2 samples, was not found in the XRD patterns, as shown in Fig. 6.

4. Analysis and Discussion

Analysis of TGA/DTA thermograms indicated that high strontium content ($x = 0.9$) prevents linear shrinkage. The dependence of composition on linear shrinkage was described as a parabolic curve with the composition $x = 0.5$ having the highest shrinkage (27%). Meixner and Cutler reported similar results where an increase in strontium levels decreased the sinterability and increased the porosity of LSM materials.

The maximum in conductivity at $x = 0.5$ correlates well to the defect chemistry of the compound. It was shown by Mizusaki and Anderson that the addition of Sr to $LaFeO_3$ creates Sr'_{La}, a charge imbalance, which must be corrected by the formation of Fe^{4+} ions or oxygen vacancies ($V_O^{\bullet\bullet}$). Therefore the highest theoretical conductivity expected by Sr addition would be $x = 0.5$ creating a maximum Fe^{4+}/Fe^{3+} ratio of 1:1. Figure 1 shows plotted data that correlates well with the

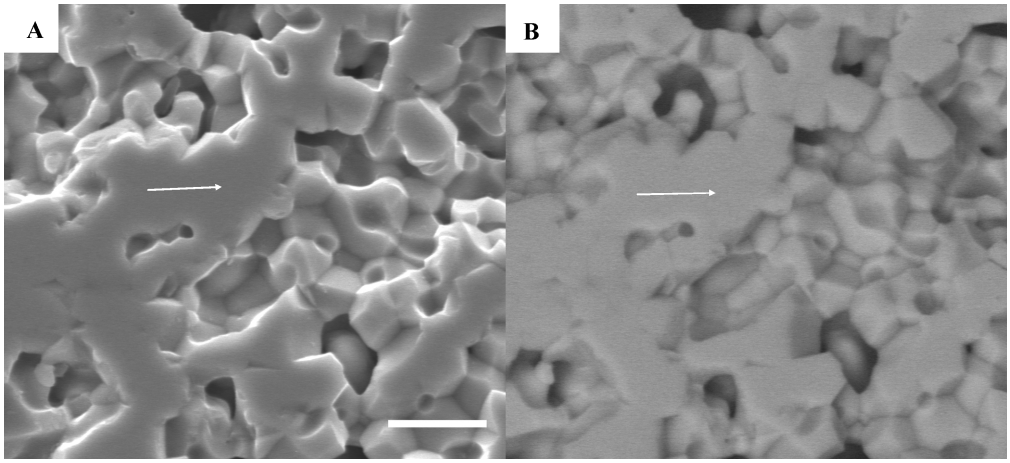

Fig. 5. Secondary (a) and backscattered electron (b) micrographs of $La_{0.5}Sr_{0.5}FeO_3$ sintered in flowing N_2 with arrows pointing towards EDS analysis areas with a 5 μm scale bar.

theoretical prediction for electrical conductivity. Equations (1) and (2) are two proposed defect equations that were used to describe the influence of sintering atmosphere on electrical conductivity, as shown in Fig. 2. Under relatively high oxygen partial pressure conditions (air and O_2), Sr'_{La} defects are compensated by holes (that form Fe^{4+}) which are the predominant charge carrier. At lower oxygen partial pressure Sr'_{La} defects are compensated by oxygen vacancies, which do not contribute to the electronic conductivity. When sintered and tested for conductivity in air the $La_{0.5}Sr_{0.5}FeO_3$ composition formed electron holes and some vacancies of oxygen, as proposed in Eqs. (1) and (2), and had a maximum electrical conductivity of 134 S/cm at 450°C, as shown in Fig. 2. Sintering in an oxygen rich environment resulted in a higher concentration of electron holes, as proposed in Eq. (2), which slightly enhanced the electrical conductivity of the material, to 147 S/cm. When sintered and tested for conductivity in a low partial pressure of oxygen atmosphere, i.e. nitrogen, the formation of additional $V_O^{\bullet\bullet}$ prevented the formation of electron holes and therefore significantly reduced the electrical conductivity, as shown in Fig. 2. The nitrogen environment also caused deterioration of the perovskite phase as found by the formation of a hygroscopic phase in $La_{0.3}Sr_{0.7}FeO_3$, which caused cracking and swelling when left in moist environments. Extending the dwell time at each measurement temperature to 1 h increased the accuracy of electrical conductivity experiments. Error in the electrical

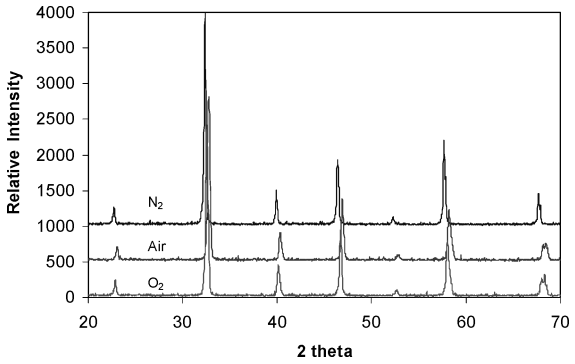

Fig. 6. Diffraction patterns of $La_{0.5}Sr_{0.5}FeO_3$ solid samples, sintered in indicated atmospheres, using Cu Kα radiation at 0.04° step and 3 sec dwell from 20 to 70° 2θ.

conductivity measurements would be caused by sample equilibration with the testing atmosphere, which would cause the material to create or fill oxygen defects and therefore lower or raise the conductivity results as measurement time is extended. Measurement time was not studied and is beyond the scope of the paper.

$$SrO + \frac{1}{2}Fe_2O_3 \xrightarrow{LaFeO_3} Sr'_{La} + Fe_{Fe} + \frac{5}{2}O_O + \frac{1}{2}V_O^{\bullet\bullet} \quad (1)$$

$$2SrO + Fe_2O_3 + \frac{1}{2}O_2(g) \xrightarrow{2LaFeO_3} 2Sr'_{La} + Fe_{Fe} + 6O_O + 2h^{\circ} \quad (2)$$

Analysis of the XRD patterns did not indicate the presence of a second phase for the air, O_2, or N_2 samples of $x = 0.5$ composition because of the small amount of second phase present. A more sensitive technique, such as transmission electron microscopy (TEM), is required to analyze the phases present.

5. Conclusions

A maximum conductivity of 352 S/cm at 550°C was measured for $La_{0.5}Sr_{0.5}FeO_3$ sintered in flowing air at 1400°C. Lower PO_2 conditions decreased the electrical conductivity below the required level for cathode operation, increased density, and decreased the apparent porosity of $La_{0.5}Sr_{0.5}FeO_3$. SEM analysis discovered a second phase that XRD could not detect due to the small volume fraction of second phase. Oxygen and air fired samples increased the porosity and had similar conductivities near 150 S/cm. PO_2 in the atmosphere was determined to have a large effect on the sintering conditions as well as electrical properties due to oxygen vacancy control and electron hole formation.

6. Future Work

The second phase will be identified using TEM with electron diffraction and EDS analysis, and 4-point thermoelectric measurements will be analyzed to study the defect chemistry and to develop further understanding of the electrical properties of LSF materials.

Acknowledgments

The authors acknowledge the financial support of the NYSTAR designated Center for Advance Ceramic Technology (CACT) at Alfred University.

References

1. N.Q. Minh, *J. Am. Ceram. Soc.*, **76**, 563 (1993).
2. P. Knauth and H.L. Tuller, *J. Am. Ceram. Soc.*, **85**, 1654 (2002).
3. J. Mizusaki, T. Sasamoto, W.R. Cannon, and H.K. Bowen, *J. Am. Ceram. Soc.*, **66**, 247 (1983).
4. S.P. Simner, J.F. Bonnett, N.L. Canfield, K.D. Meinhardt, V.L. Sprenkle, and J.W. Stevenson, *Electrochemical and Solid-State Letters*, **5**, A173 (2002).
5. J. Mizusaki, *Solid State Ionics*, **52**, 79 (1992).
6. H.U. Anderson, *Solid State Ionics*, **52**, 33 (1992).
7. M.C. Kim, S. Ja Park, H. Haneda, J. Tanaka, and S. Shirasaki, *Solid State Ionics*, **40–41**, 239 (1990).
8. D.L. Meixner and R.A. Cutler, *Solid State Ionics*, **146**, 273 (2002).
9. O. Yamamoto, Y. Takeda, R. Kanno, and M. Noda, *Solid State Ionics*, **22**, 241 (1987).
10. P.J. Gellings and H.J.M. Bouwmeester, *The CRC Handbook of Solid State Electrochemistry* (CRC Press, Boca Raton, 1997), p. 415.
11. R.J. Bell, G.J. Millar, and J. Drennan, *Solid State Ionics*, **131**, 211 (2000).
12. B.C. LaCourse, *The Effect of Processing Variables on the Reproducibility of PTCR $BaTiO_3$* (Alfred University, Alfred, 1993), p. 30.
13. S.E. Dann, D.B. Currie, M.T. Weller, M.F. Thomas, and A.D. Al-Rawwas, *J. Solid State Chem.*, **109**, 134 (1994).
14. F.C. Raszewski, *Chemical Synthesis and Characterization of High Temperature $La_xSr_{1-x}FeO_{3-\delta}$ Ceramic Electrodes* (Alfred University, Alfred, 2003), p. 9.